Michelle B. Trevino,[1] Yui Machida,[1] Daniel R. Hallinger,[1] Eden Garcia,[1] Aaron Christensen,[1] Sucharita Dutta,[2] David A. Peake,[3] Yasuhiro Ikeda,[4] and Yumi Imai[1]

Perilipin 5 Regulates Islet Lipid Metabolism and Insulin Secretion in a cAMP-Dependent Manner: Implication of Its Role in the Postprandial Insulin Secretion

Diabetes 2015;64:1299–1310 | DOI: 10.2337/db14-0559

Elevation of circulating fatty acids (FA) during fasting supports postprandial (PP) insulin secretion that is critical for glucose homeostasis and is impaired in diabetes. We tested our hypothesis that lipid droplet (LD) protein perilipin 5 (PLIN5) in β-cells aids PP insulin secretion by regulating intracellular lipid metabolism. We demonstrated that PLIN5 serves as an LD protein in human islets. In vivo, *Plin5* and triglycerides were increased by fasting in mouse islets. MIN6 cells expressing PLIN5 (adenovirus [Ad]-PLIN5) and those expressing perilipin 2 (PLIN2) (Ad-PLIN2) had higher [^{3}H]FA incorporation into triglycerides than Ad-GFP control, which support their roles as LD proteins. However, Ad-PLIN5 cells had higher lipolysis than Ad-PLIN2 cells, which increased further by 8-Br-cAMP, indicating that PLIN5 facilitates FA mobilization upon cAMP stimulation as seen postprandially. Ad-PLIN5 in islets enhanced the augmentation of glucose-stimulated insulin secretion by FA and 8-Br-cAMP in G-protein–coupled receptor 40 (GPR40)- and cAMP-activated protein kinase–dependent manners, respectively. When PLIN5 was increased in mouse β-cells in vivo, glucose tolerance after an acute exenatide challenge was improved. Therefore, the elevation of islet PLIN5 during fasting allows partitioning of FA into LD that is released upon refeeding to support PP insulin secretion in cAMP- and GPR40-dependent manners.

The loss of functional β-cell mass is a fundamental defect in diabetes (1), because glucose homeostasis depends on basal insulin secretion to maintain fasting glucose and robust postprandial (PP) insulin release to prevent postmeal hyperglycemia. Importantly, PP hyperglycemia is an early defect in diabetes, a key contributor in macrovascular complications, and a major barrier for optimal glycemic control in patients with diabetes (2–6). Thus, understanding pathways that support PP insulin secretion has significant implications for diabetes management.

Fatty acids (FA) support PP insulin secretion by acutely augmenting insulin release (5,6) by activation of cell surface G-protein–coupled receptor 40 (GPR40) and the generation of intracellular FA metabolites (7,8). Interestingly, depletion of FA during fasting impairs subsequent insulin secretion (9). This could be partly due to the necessity of FA to support basal respiration during fasting (10) but also may reflect the contribution of intracellular FA metabolism preceding meals for PP insulin secretion. However, a mechanism by which intracellular lipids optimize PP insulin secretion is undefined.

The perilipin family (PLIN1 through 5) of lipid droplet (LD) proteins resides around intracellular neutral lipid cores consisting of triglycerides (TG) and cholesterol esters and governs the metabolism of intracellular lipid

[1]Department of Internal Medicine, Strelitz Diabetes Center, Eastern Virginia Medical School, Norfolk, VA
[2]Leroy T. Canoles Cancer Research Center, Eastern Virginia Medical School, Norfolk, VA
[3]Thermo Fisher Scientific, San Jose, CA
[4]Department of Molecular Medicine, Mayo Clinic, Rochester, MN
Corresponding author: Yumi Imai, imaiy@evms.edu.

Received 8 April 2014 and accepted 4 November 2014.
This article contains Supplementary Data online at http://diabetes.diabetesjournals.org/lookup/suppl/doi:10.2337/db14-0559/-/DC1.

depots (11,12). PLIN subtype expression is tissue-specific and regulated by the metabolic state of cells (12). PLIN1 is highly expressed in adipocytes, where it prevents lipolysis at the basal state but supports robust lipolysis in a cAMP-dependent protein kinase (PKA) activated manner through its interaction with hormone-sensitive lipase (HSL) and CGI-58, an activator of adipose TG lipase (ATGL) (11).

PLIN2 is ubiquitously expressed including mouse and human islets and regulates intracellular lipid metabolism and insulin secretion (13,14). The knockdown of *Plin2* impaired FA-induced glucose-stimulated insulin secretion (GSIS) in MIN6 cells (14). Although unexplored in β-cells, PLIN5 has unique features among PLINs that may be applicable to islet lipid metabolism and insulin secretion. PLIN5 is highly expressed in tissues where FA serves as a fuel, such as heart, type I skeletal muscles, and brown adipose tissue (BAT), and is upregulated in the liver and heart by fasting (15–17). A unique COOH-terminal region that tethers PLIN5 to mitochondria leads to the proposition that PLIN5 facilitates FA transfer from LD to mitochondria for oxidation (18) or protects cells from oxidative stress through reductions in FA oxidation (19). Two seemingly opposite functions proposed are based on both increase and decrease in FA oxidation after the modulation of PLIN5 expression in various models (16,18,20–22). Multifaceted functions of PLIN5 are likely conferred by its interaction with ATGL and CGI-58 (22–24) and its ability to increase lipolysis with PKA stimulation (22), altering PLIN5 functions depending on the cellular environment. Given actions of PLIN5 in other metabolic tissues in lipid mobilization, we addressed whether PLIN5 in β-cells plays a critical role in supporting PP insulin secretion through its regulation of lipid metabolism.

RESEARCH DESIGN AND METHODS

Animal Studies

Experiments were in accordance with the Eastern Virginia Medical School Institutional Animal Care and Use Committee guidelines. Male C57Bl/6N (Bl6; Harlan Laboratories, Indianapolis, IN; or Charles River, Wilmington, MA) mice (12–16 weeks old) had free access to chow except when being fasted up to 24 h. Mouse islets were obtained as described (25). Serum analyses measuring TG (Stanbio Laboratories, Boerne, TX), β-hydroxybutyrate (Stanbio), nonesterified FA (Wako Chemicals, Richmond, VA), and insulin (ALPCO Diagnostics, Salem, NH) were performed according to manufacturers' instructions.

Human Islets

Human islets from nondiabetic donors provided by the Integrated Islet Distribution Program and Prodo Laboratories were incubated in 10% FBS CMRL 1066 medium at 37°C in 5% CO_2 overnight to recover from shipping. For RNA measurements, islets were incubated additional 24 h in CMRL 1066 with or without 0.5 mmol/L oleic acid (OA) or palmitic acid (PA) conjugated to 1% FA-free human albumin.

Immunofluorescent Analyses

Partially dispersed human islets were fixed in 3% paraformaldehyde for 15 min, permeabilized in 0.1% Tween PBS for 15 min, blocked with 2% BSA PBS, and incubated with primary and secondary antibodies (Ab) for 1 h each in 1% BSA PBS, followed by 1 μg/mL DAPI for 2 min. For Fig. 1*A–C*, islets were treated as above using Bodipy 488 (Invitrogen, Carlsbad, CA) during secondary Ab incubation. For Bodipy 558/568 C_{12} labeling, islets were incubated in CMRL 1066 plus 0.5 mmol/L OA and 0.2 μg/μL Bodipy 558/568 C_{12} for 72 h before immunostaining. Paraffin-embedded pancreata were analyzed as described (14). Primary Abs were guinea pig anti-PLIN5 (Progen Biotechnik, Heidelberg), guinea pig anti-PLIN2 (Fitzgerald, Acton, MA) both at 1:100, and rabbit anti-insulin (Santa Cruz Biotechnology, Santa Cruz, CA) at 1:200. Secondary Abs were goat anti-guinea pig-DyLight 488 and goat anti-rabbit-DyLight 594 (Jackson Immunology, West Grove, PA) at 1:1,000. Images were captured with an Axio Observer Z.1 fluorescent microscope (Carl Zeiss) using AxioVision Release 4.7.

Quantitative PCR

Total RNA prepared using Qiagen RNeasy kit (Qiagen, Valencia, CA) was transcribed to cDNA as described (14,25). Gene expressions were analyzed using ABI TaqMan commercial primers (Applied Biosystems, Foster City, CA), taking β-actin as an internal standard, as described (14,25).

Western Blotting

Western blotting was performed using 20 to 40 μg/lane protein with visualization by chemiluminescence and densitometric analyses by ImageJ software, as described (16). Primary Abs were guinea pig anti-PLIN5, guinea pig anti-PLIN2, and rabbit anti-GAPDH (Cell Signaling Technology, Inc., Danvers, MA) all at 1:1,000. Secondary Abs were horseradish peroxidase–conjugated goat anti-guinea pig-IgG or anti-rabbit-IgG (Santa Cruz Biotechnology) at 1:5,000.

Mass Spectrometry–Based TG Analyses

Lipids from islets were extracted as described (14) and analyzed on the Q Exactive Orbitrap (Thermo Scientific, San Jose, CA), a high-resolution accurate mass spectrometry (MS) platform, via liquid chromatography–tandem MS (MS/MS). The column conditions and buffers followed a protocol that previously identified lipids, including TG (26,27). Briefly, an high-performance liquid chromatography C18 Polar Ascentis Express column (Supelco, 2.1 × 150 mm; 2.7 μm) separated lipid before lipid detection on the Q Exactive. Lipid information was collected at 70,000 resolution on the Q Exactive for full MS data (Supplementary Fig. 1*A*) and at 35,000 resolution for MS/MS data (Supplementary Fig. 1*B*) in positive ion mode. Positive ion mode was shown to optimize the detection of TG by the Q Exactive (27). Peaks in a raw data file of product ion scan (MS/MS, Supplementary Fig. 1*B*) were assessed using the Lipid Search algorithm (MKI, Tokyo, Japan), a comprehensive database of more than

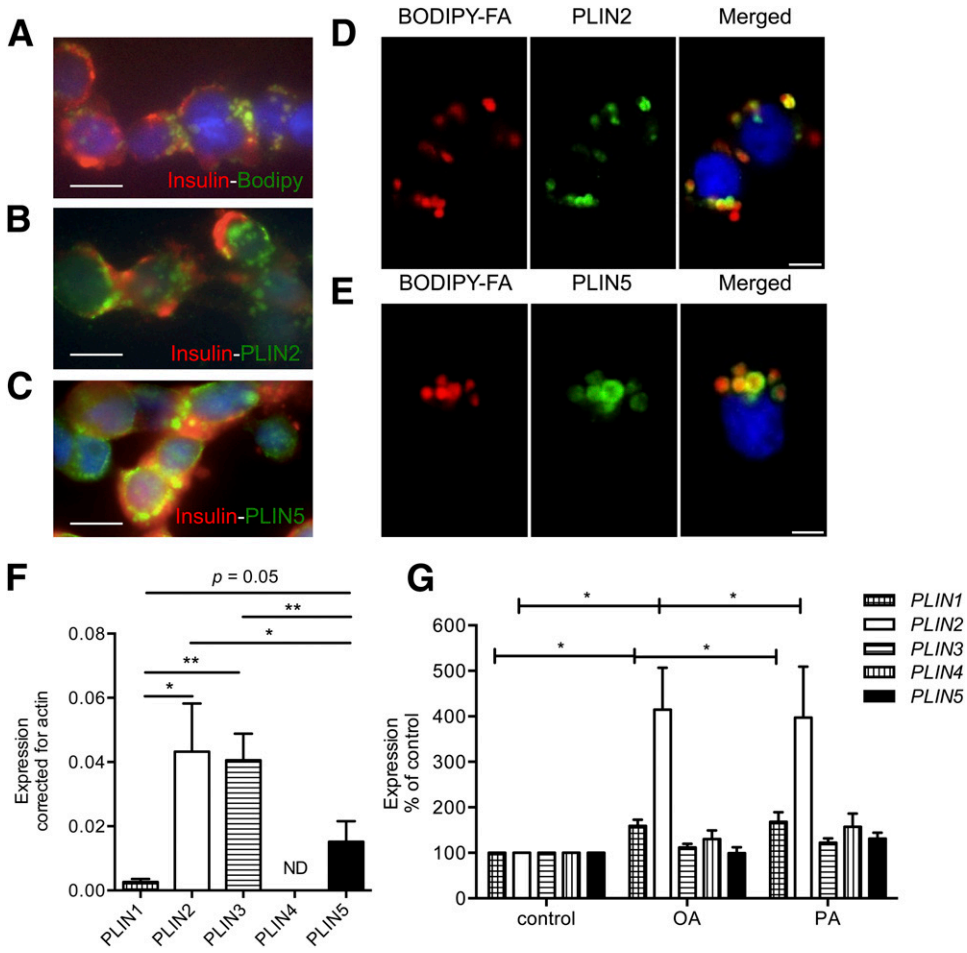

Figure 1—PLIN5 is an LD protein in human β-cells. Dispersed human islets immunostained with insulin (red) and Bodipy 488 (*A*), PLIN2 (*B*), or PLIN5 (*C*) in green. Dispersed human islets metabolically labeled to show TG with Bodipy-FA 558/568 C_{12} (red) were costained with PLIN2 (*D*) or PLIN5 (*E*) in green. Merged images include blue DAPI-stained nuclei. *A–E*: Scale bar, 10 μm. *F*: *PLIN* mRNA quantified in whole human islets cultured in 10% FBS medium. Data are means ± SEM; n = 4–12. $^*P < 0.05$, $^{**}P < 0.01$. *G*: *PLIN* mRNA quantified in whole human islets cultured overnight in media without (control) or with 0.5 mmol/L OA or PA. Data are means ± SEM; n = 4–8. $^*P < 0.05$.

10^6 lipid species. Each fragmented lipid (MS/MS) was matched to a fragmentation library and predicted retention time to determine the FA chain composition of TG (Supplementary Fig. 1*B* and *C*) (27). For relative quantification of the TG identified, the integrated precursor-extracted ion chromatograms are calculated based on the high-resolution accurate mass information, and area under the curve of relative abundance in the integrated precursor extracted ion chromatograms was used as TG area (Supplementary Fig. 1*D*). The mass tolerance was set to 5 ppm for the precursor mass. Total TG peak area for fed or fasted islets was defined as a sum of the TG areas obtained as above for all TG identified in each islet specimen (Supplementary Table 1 and Table 2) expressed in log10 and normalized to islet protein contents.

Adenovirus Transduction

MIN6 cells were transduced at 20 plaque-forming units (pfu) per cell of adenovirus (Ad) expressing GFP, mouse PLIN5 (Ad-PLIN5), or mouse PLIN2 (Ad-PLIN2), all from Vector BioLabs (Philadelphia, PA), for 1 h in serum-free DMEM (22.2 mmol/L glucose) and cultured overnight in 10% FBS DMEM, followed by incubation in 3 mmol/L glucose DMEM, with or without 0.5 mmol/L OA, conjugated to 1% FA-free BSA for overnight at 37°C in 5% CO_2 before quantitative (q)PCR, Western blot, and [^{3}H]OA labeling. Freshly isolated mouse islets were transduced with Ad at 2×10^4 pfu/islet in serum-free RPMI 1640 (10 mmol/L glucose) for 1 h, then incubated with the addition of 10% FBS at 37°C in 5% CO_2 overnight before analyses.

[^{3}H]OA Labeling

After incubation with 1.2 Ci/mL [^{3}H]OA (specific activity 10 mCi/mol; NEN, Boston, MA) in DMEM with 0.5 mmol/L OA for 5 h, [^{3}H] incorporation into lipids and H_2O was determined in MIN6 cells as described (14). Briefly, [^{3}H]OA incorporation to cellular TG was determined by Folch extraction, followed by thin-layer chromatography. Production of [^{3}H]H_2O was measured in medium after

trichloroacetic acid precipitation (16). Lipolysis was measured as reduction of [^{3}H]OA-labeled TG in MIN6 cells prelabeled with [^{3}H]OA for 18 h incubated in isotope-free 3 mmol/L glucose DMEM with 0.5 mmol/L OA and 9.5 μmol/L triacsin C (Enzo Life Sciences, Plymouth Meeting, PA) to prevent reincorporation of [^{3}H]OA to TG (16). Data were normalized to cellular protein contents.

GSIS

After 1 h preincubation in glucose-free Krebs-Ringer buffer (KRB), MIN6 cells (9×10^5 cells/12 well) or mouse islets (10 islets/0.5-mL tube) transduced with Ad were incubated for 1 h in KRB containing glucose (3 or 16.7 mmol/L), 0.5 mmol/L PA, 1 mmol/L 8-Br-cAMP, and 1 μmol/L nifedipine (Sigma-Aldrich). Some islets were treated for 30 min with 1 μmol/L GW1100 (Cayman Chemical, Ann Arbor, MI) before PA treatment or 30 min with 20 μmol/L H-89 (Cell Signaling, Beverly, MA) before 8-Br-cAMP. Insulin secreted into KRB and insulin contents were measured with insulin ELISA (Mercodia, Inc., Winston-Salem, NC) as described (25). GSIS were expressed per 9×10^5 cell (MIN6 cells), per 10 islets (mouse islets), except for Supplementary Fig. 5*E*, where 1 islet/well was used.

Ad-Associated Virus Serotype 8 Construct and Transduction

Ad-associated virus (AAV) serotype 8 vectors carrying cDNA for GFP (AAV-GFP) and mouse PLIN5 (AAV-PLIN5) under mouse insulin 2 promoter were custom made at Penn Vector Core (Philadelphia, PA). AAV-GFP and AAV-PLIN5 were delivered to 12-week-old male Bl6 mice intraperitoneally at 4×10^{11} viral genome per mouse. Intraperitoneal glucose tolerance tests (IPGTT; 1.5 mg/g body weight glucose after overnight fasting) and insulin tolerance tests (ITT, 0.75 mIU/g body weight human regular insulin after 4 h fasting) were performed by obtaining tail blood and using a handheld glucometer as described (25). The tail vein was used to obtain blood for serum analyses. For the exenatide experiment, overnight fasted mice were given 0.01 μg/g body weight Byetta (Amylin Pharmaceuticals, San Diego, CA) intraperitoneally 10 min before the IPGTT.

Statistics

Studies were performed at least three times. Data are presented as means ± SEM. Differences of numeric parameters between two groups were assessed with Student *t* tests or the Mann-Whitney test, and those for multiple group comparisons used one-way ANOVA (Tukey or Dunnett post hoc). Two-way ANOVA determined significance for IPGTT and ITT. $P < 0.05$ was considered significant.

RESULTS

PLIN5 Is an LD Protein in β-Cells

Human β-cells were analyzed by immunostaining for LD marker Bodipy 488 (Fig. 1*A*), PLIN2 (Fig. 1*B*), or PLIN5 (Fig. 1*C*), along with insulin. As reported (28), human islets have large LD, shown as green punctate Bodipy 488 staining in insulin-positive cells (Fig. 1*A*). Abundant punctate staining within insulin-positive cells implicates PLIN2 and PLIN5 as LD proteins in β-cells (Fig. 1*B* and *C*). These punctate structures are confirmed as TG containing LD through metabolic labeling of human islets with Bodipy-FA 558/568 C_{12}, an FA-conjugated fluorescent marker incorporated into TG (29). Importantly, PLIN2 and PLIN5 were both adjacent to LD labeled with Bodipy-FA 558/568 C_{12} in human islets (Fig. 1*D* and *E*). When PLIN expressions were compared in human islets, *PLIN5* was the third most abundant PLIN, behind *PLIN2* and *PLIN3*, and was expressed more than *PLIN1* whose presence in islets was previously reported (30) (Fig. 1*F*). There was no correlation between donors' BMI and *PLIN2* or *PLIN5* expression (Supplementary Fig. 2*A* and *B*). Overnight FA incubation increased *PLIN2* expression, as we reported (14), but did not change *PLIN5, PLIN3,* or *PLIN4* expression, suggesting differential *PLIN* expressions in human islets (Fig. 1*G*). *PLIN1* showed a small but significant increase by FA incubation, which might include contribution from nonendocrine cells.

Plin5 Is Upregulated in Fasted Islets and Remains Elevated During the PP State

The differential regulation of *Plin2* and *Plin5* expression was also observed in mouse islets. The high-fat diet did not alter *Plin5* but increased *Plin2* expression in mouse islets (Supplementary Fig. 2*C* and *D*). In contrast, *Plin5* but not *Plin2* (Fig. 2*A* and *B*) or *Plin3* (data not shown) expression was increased in islets from fasted mice, implicating PLIN5 may play a role in the regulation of lipid metabolism during fasting that is known to affect insulin secretion (9). Among metabolic tissues, islets increased LD-related gene expression along with liver, indicating active remodeling of LD in fasted islets (Fig. 2*A*–*D*). Fasting increased islet *Plin5* to 10.1-fold compared with 8.3-fold in liver and 4.7-fold in skeletal muscle over fed tissues (Fig. 2*A*). Western blot confirmed increased PLIN5 protein in fasted islet and liver (Fig. 2*E*). *Plin2* expression was increased only in liver (Fig. 2*B*), with a mild but significant reduction in BAT. Notably, diglyceride acyltransferases (DGAT1 and DGAT2), enzymes responsible for the last step of TG synthesis, also showed differential regulation in a tissue-specific manner. *Dgat2* mRNA was increased in fasted islets, whereas *Dgat1* was predominantly increased in fasted liver (Fig. 2*C* and *D*). Structural and functional distinctions of two DGATs (31) and PLINs likely support tissue-specific lipid metabolism during fasting in liver and islets. The intensity of PLIN5 immunostaining in insulin-positive cells was enhanced in 24-h fasted mouse pancreas, indicating that β-cells are responsible for the rise in mRNA (Fig. 2*A*) and protein (Fig. 2*E*) in fasted mouse islets (Fig. 2*F*). Nonpunctate staining of PLIN5 reflects smaller-sized LD in mice compared with human β-cells seen with Bodipy 558/568 C_{12} staining (Supplementary Fig. 2*E*). Species difference was also noted, with higher capacity of TG formation in human

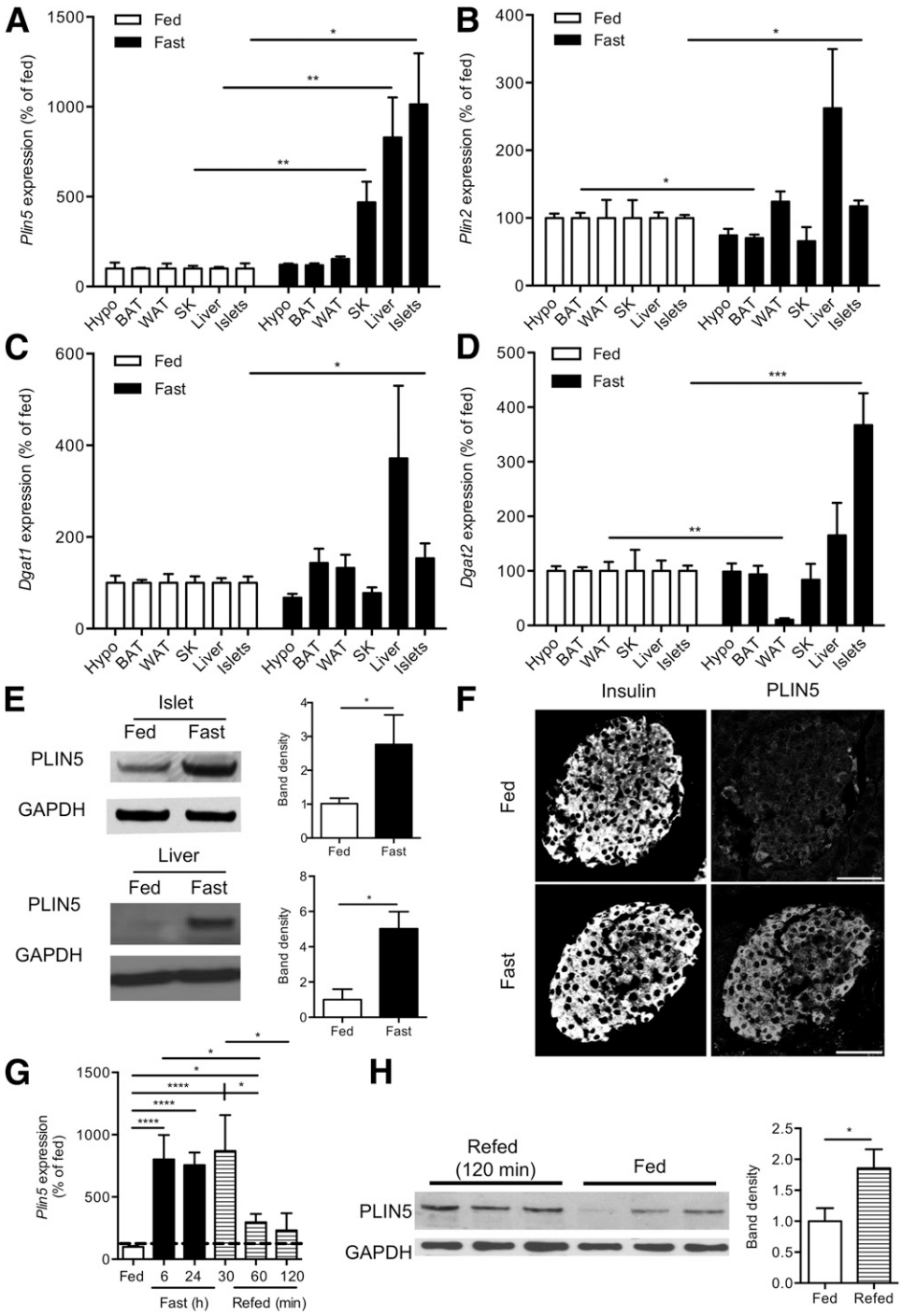

Figure 2—Fasting upregulates PLIN5 in mouse islets. Quantitative PCR of *Plin5* (*A*), *Plin2* (*B*), *Dgat1* (*C*), and *Dgat2* (*D*) in hypothalamus (hypo), BAT from the intrascapular depot, epididymal white adipose tissue (WAT), quadriceps femoris muscle (SK), liver, and islets in C57Bl/6 mice fed or fasted 24 h expressed, taking the average expression levels of corresponding tissues from fed mice as 100% and using β-actin as internal control. *E*: Western blot of PLIN5 in islets and liver from fed and fasted mice. Band density was expressed as the average expression levels of corresponding tissues from fed mice as 1, using GAPDH as the internal control. *F*: Pancreatic sections from fed and fasted mice immunostained for insulin (left) and PLIN5 (right). Scale bar, 40 μm. *G*: Expression of *Plin5* in islets from mice fed chow (fed), without chow for 6 and 24 h (fast), and fed for 30 min, 60 min, and 120 min after 24 h fasting (refed) expressed as in *A–D*. *H*: Western blot of PLIN5 in islets fed or refed for 120 min expressed as in *E*. Data are means ± SEM; n = 4–9. **P* < 0.05, ***P* < 0.01, ****P* < 0.001; *****P* < 0.0001.

compared with mouse islets (Supplementary Fig. 2*F*). To determine whether the increase in PLIN5 in fasted mouse islets is associated with TG accumulation, we used a high-resolution accurate mass platform, the Q Exactive Orbitrap, that allows identification and quantification of wide range of TG species (Supplementary Fig. 1*A–D*) (27). More than 200 TG species were identified in fed and fasted mouse islets, including 201 that were observed

only in fasted islets (Supplementary Table 1). The rest of the TG species were increased in fasted over fed islets (ratio over 1; Supplementary Table 2), resulting in a significant increase for fasted islets of total TG area value determined as in RESEARCH DESIGN AND METHODS (10.3 ± 0.3 in fasted vs. 6.32 ± 0.40 in fed islets, $n = 4$, $P < 0.001$). We did not identify TG species that are only found in fed islets in the current assay. Our data indicate that mouse islets accumulate TG during fasting as do the heart and liver (20). These data are concordant with the rise in PLIN5 in fasted islets (Fig. 2*E* and *F*), because PLIN5 has been shown to promote the formation of LD in other cells (19).

Next, expressions of lipid metabolic genes in islets during refeeding were assessed. Marked increases in serum insulin and suppression of β-hydroxybutyrate characterized PP status in mice fed for 60 min after 24 h fasting (Supplementary Fig. 3*A*–*F*). Among genes related to LD metabolism, *Plin5* expression was increased after as short as 6 h of fasting, remained elevated at 30 min after refeeding, and was slow to decline in islets, staying above levels in the fed group at 120 min after refeeding (Fig. 2*G*). Reductions in blood glucose and insulin verify 6-h fasting statuses (Supplementary Fig. 3*G*–*I*). Western blotting confirmed elevated PLIN5 protein at 120 min after refeeding compared with islets of fed mice (Fig. 2*H*). *Plin2* and a key enzyme for FA oxidation, acyl-CoA thioesterase 2 (*Acot2*), showed significant reductions by 120 min, and *Dgat2* was near baseline as well (Supplementary Fig. 3*J*–*L*). Collectively, the dramatic rise of islet PLIN5 and TG during fasting and the slow reduction of islet PLIN5 during refeeding implicates PLIN5 as a potential regulator of lipid metabolism during fasting and also postprandially in β-cells.

PLIN5 Uniquely Regulates Lipid Metabolism in β-Cells

To determine how increased expression of PLIN5 affects β-cell lipid metabolism compared with PLIN2, both PLINs were expressed using an Ad in MIN6 cells to achieve a similar increase (approximately twofold) in [^{3}H]OA incorporation into TG (Fig. 3*A*). Endogenous expression of PLIN5 was low in MIN6 cells (Fig. 3*B*). Similar to *PLIN5* expression in human islets (Fig. 1*G*), overnight OA incubation did not alter PLIN5 protein levels in the PLIN5 or GFP control group (Fig. 3*B*). In contrast, OA increased PLIN2 levels in the Ad-PLIN2 and Ad-GFP groups (Supplementary Fig. 4*A*), which likely reflects upregulation of *Plin2* mRNA by FA in β-cells (14) and the prevention of ubiquitin-mediated degradation of PLIN2 by FA (32,33). The modest increase of PLIN2 in Ad-PLIN5 cells is also likely driven by PLIN2 stabilization by increased LD formation in Ad-PLIN5 cells (Fig. 3*C*). Thus, the increases in

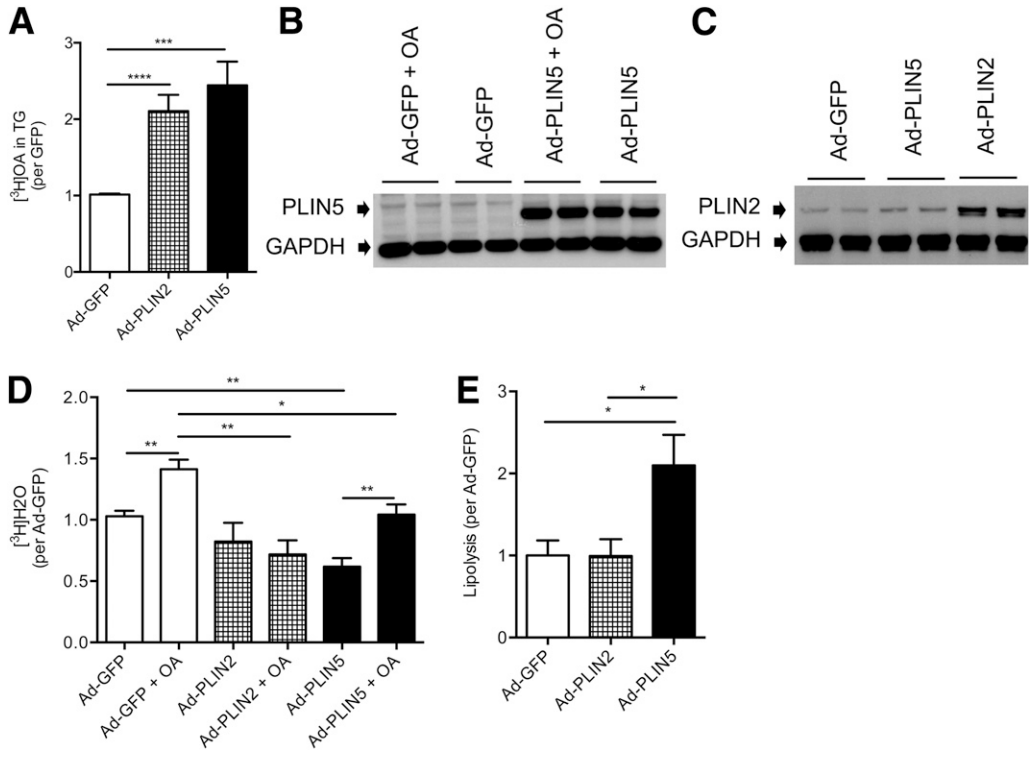

Figure 3—Upregulation of PLIN5 uniquely regulates lipid metabolism in MIN6 cells. MIN6 cells were transduced with Ad to express PLINs or GFP. *A*: The incorporation of [^{3}H]OA to TG was compared by metabolic labeling of transduced MIN6 cells with [^{3}H]OA. Western blot of PLIN5 in Ad-GFP and Ad-PLIN5 MIN6 cells with and without 0.5 mmol/L OA (*B*) and PLIN2 expression in Ad-GFP, Ad-PLIN5, and Ad-PLIN2 MIN6 cells along with GAPDH as loading control (*C*). The production of [^{3}H]H_2O (*D*) and lipolysis (*E*) during 4 h was compared by metabolic labeling of transduced MIN6 cells with [^{3}H]OA. Data are corrected for the specific activity of [^{3}H]OA, adjusted for protein/well thereafter expressed relative to the average of Ad-GFP cells. Data are means ± SEM; $n = 3$–7. *$P < 0.05$, **$P < 0.01$, ***$P < 0.001$, ****$P < 0.0001$.

PLIN2 protein but not mRNA that we reported in fasted islets (14) are likely driven by the increase of PLIN5 in fasted islets (Fig. 2*A*, *E*, and *F*). However, elevating PLIN2 expression did not alter PLIN5 protein levels in Ad-PLIN2 cells (Supplementary Fig. 4*B*). The overexpression of PLIN5 but not PLIN2 in MIN6 cells altered expressions of several genes in lipid pathways, implying that each PLIN has distinct functions in the β-cell environment (Supplementary Fig. 4*C*).

Next, metabolic handling of exogenous FA was compared among Ad-PLIN5, Ad-PLIN2, and Ad-GFP cells. Expectedly, OA preloading increased subsequent OA oxidation measured as $[^3H]H_2O$ production in Ad-GFP cells (Fig. 3*D*). In Ad-PLIN2 cells, $[^3H]H_2O$ production was comparable to Ad-GFP cells without OA preloading but failed to increase after OA loading (Fig. 3*D*). In contrast, $[^3H]H_2O$ production in Ad-PLIN5 cells was reduced at baseline but increased significantly after OA loading but remained lower than in OA-loaded Ad-GFP cells (Fig. 3*D*). Although [^{3}H]OA incorporation into TG was increased to comparable levels in Ad-PLIN2 and Ad-PLIN5 cells (Fig. 3*A*), PLIN5 but not PLIN2 expression promoted lipolysis (Fig. 3*E*). PLIN5 overexpression did not alter incorporation of [^{3}H]OA to other lipid species (Supplementary Fig. 4*D*). Thus, PLIN5 demonstrates the hallmark feature of an LD protein with increased incorporation of [^{3}H]OA into TG but affects gene expression and lipolysis more prominently compared with PLIN2 in MIN6 cells.

PLIN5 Enhances the Acute Augmentation of GSIS by PA Partly Through a GPR40 Pathway

The effects of higher PLIN5 and PLIN2 expressions on the acute augmentation of GSIS by PA were compared. Ad-mediated expression of GFP, PLIN5, or PLIN2 did not interfere with GSIS in MIN6 cells (Fig. 4*A*). As expected, PA acutely potentiated GSIS in Ad-GFP control cells (Fig. 4B), which was further augmented in Ad-PLIN5 cells (Fig. 4*B*) but not in Ad-PLIN2 cells (Supplementary Fig. 5*A*). As in MIN6 cells, increasing PLIN5 expression in mouse islets enhanced PA-induced GSIS compared with Ad-GFP islets (Fig. 4*C*). Transduction by neither Ad-GFP nor Ad-PLIN5 altered islet insulin contents (Supplementary Fig. 5*B*). The activation of cell-surface GPR40 plays a major role in the acute augmentation of GSIS by PA (7). Interestingly, despite the intracellular location of PLIN5, the acute PA augmentation of GSIS in Ad-PLIN5 islets was highly sensitive to GW1100, a GPR40 antagonist, and reduced GSIS in the presence of PA and GW1100 to levels comparable with those in Ad-GFP islets (Fig. 4*C*). GPR40 receptor (*ffar1*) expression was unaltered by overexpression of PLIN5 seen in Ad-PLIN5 islets (Supplementary Fig. 5*C*).

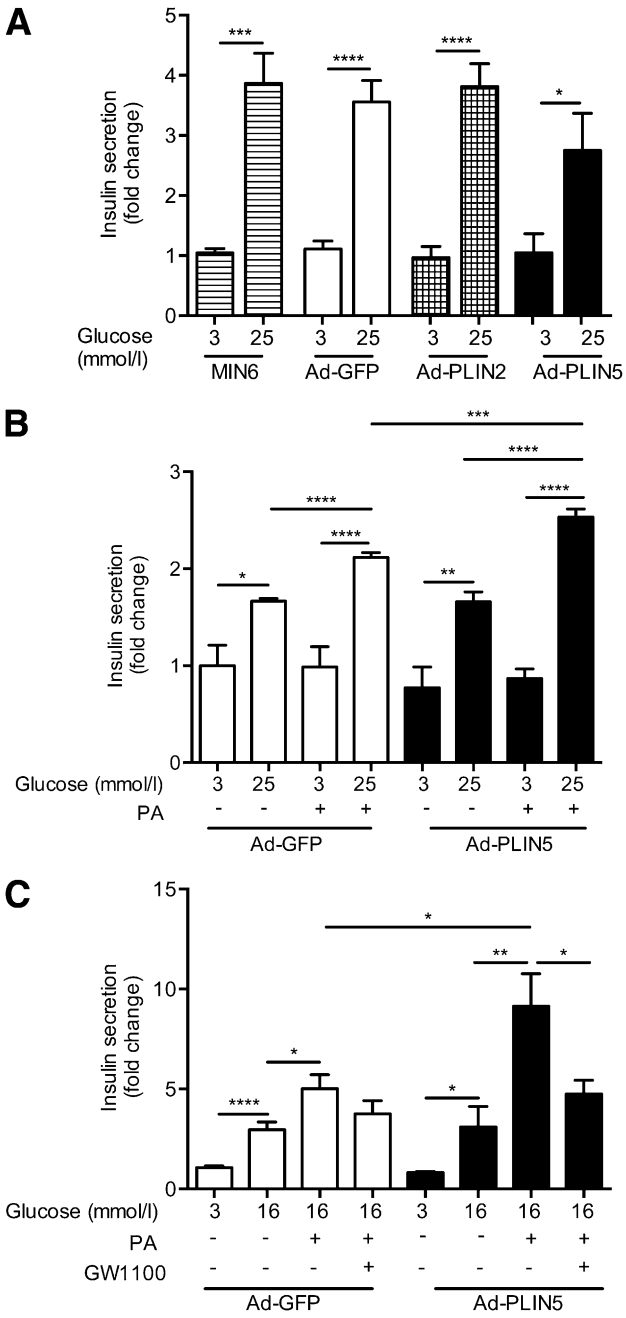

Figure 4—Upregulation of PLIN5 increases acute augmentation of GSIS by PA in MIN6 cells and mouse islets. *A*: GSIS of untransduced MIN6 cells and those transduced with Ad-GFP, Ad-PLIN5, or Ad-PLIN2. Data are means ± SEM; n = 6–9. *B*: GSIS with or without 0.25 mmol/L PA in Ad-PLIN5 MIN6 cells compared with Ad-GFP control. Data are means ± SEM; n = 6–9. *C*: GSIS with or without 0.25 mmol/L PA and 1 μmol/L GW1100, GPR40 antagonist, in Ad-PLIN5 vs. Ad-GFP mouse islets. Data expressed as the fold change taking GSIS of Ad-GFP at 3 mmol/L glucose (*A* and *C*) or at 25 mmol/L glucose (*B*) as 100%. Data are means ± SEM; n = 19–21. $^*P < 0.05$, $^{**}P < 0.01$, $^{***}P < 0.001$, $^{****}P < 0.0001$.

cAMP Analog Increased Lipolysis and Augmented GSIS in a PKA-Dependent Manner in Ad-PLIN5–Transduced Insulin-Secreting Cells

PLIN5 was shown to interact with ATGL (22,24), a key enzyme that initiates lipolysis, and increased lipolysis with activated cAMP signaling in AML12 and CHO cells (22). Although β-cell lipolysis is proposed to support stimulus-secretion coupling in β-cells (8), regulators of lipolysis in β-cells are poorly understood. Considering the slow reduction of *Plin5* expression in islets during

refeeding (Fig. 2*G*), when cAMP signaling is increased in islets (34), we addressed whether the expression of PLIN5 alters lipolysis and GSIS in response to 8-Br-cAMP in β-cells. 8-Br-cAMP increased the release of [^{3}H]OA from TG in Ad-PLIN5 MIN6 cells (Fig. 5*A*). In contrast, lipolysis in Ad-GFP did not respond to 8-Br-cAMP, likely reflecting low levels of endogenous PLIN5 in MIN6 cells. Remarkably, Ad-PLIN5 islets showed significant potentiation of GSIS upon 8-Br-cAMP treatment compared with Ad-GFP islets in a PKA-dependent manner, as PKA inhibitor H89 ablated the 8-Br-cAMP effect in Ad-GFP and Ad-PLIN5 islets (Fig. 5*B*). In contrast, GSIS with 8-Br-cAMP in Ad-PLIN2 islets was comparable to Ad-GFP control islets, indicating that PLIN5 but not PLIN2 responds to cAMP signaling of GSIS in insulin-secreting cells (Supplementary Fig. 5*D*). Because both GPR40 and cAMP signaling in β-cells raises $[Ca^{2+}]_i$ (35,36), we tested whether GSIS potentiation by PA and 8-Br-cAMP requires the activation of voltage-dependent Ca channel. The augmentation of GSIS by both treatments was blocked by nifedipine in Ad-PLIN5 islets indicating their dependence on the voltage-dependent Ca channel (Supplementary Fig. 5*E*).

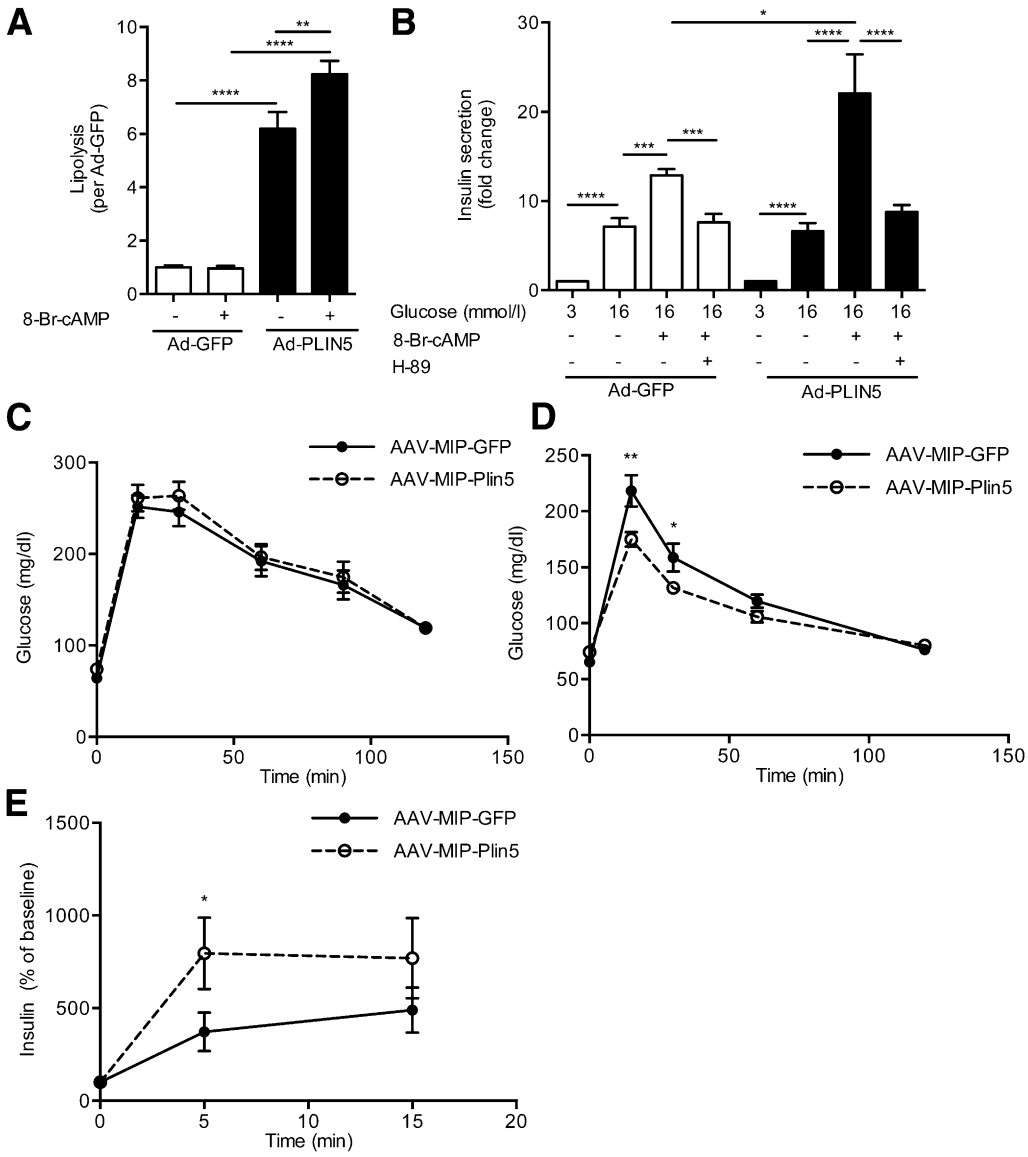

Figure 5—Upregulation of PLIN5 in β-cells enhances the augmentation of GSIS by the cAMP pathway in culture and in vivo. *A*: Lipolysis during 2 h was compared in Ad-GFP– and Ad-PLIN5–transduced MIN6 cells with or without 1 mmol/L 8-Br-cAMP. Data are means ± SEM; $n = 3$ of a representative experiment out of three. *B*: GSIS with or without 1 mmol/L 8-Br-cAMP and 20 μmol/L H-89, a PKA inhibitor, measured in Ad-PLIN5–transduced mouse islets compared with Ad-GFP control. Data are means ± SEM; $n = 15$–18. IPGTT of AAV-PLIN5 and AAV-GFP control mice without (*C*) or with (*D*) pretreatment by exenatide (0.01 μg/g body weight). Data are means ± SEM; $n = 9$–11. $^*P < 0.05$, $^{**}P < 0.01$, $^{***}P < 0.001$, $^{****}P < 0.0001$. *E*: Serum insulin during IPGTT in AAV-PLIN5 and AAV-GFP control mice pretreated by exenatide as in *D*. Data are means ± SEM; $n = 5$–7. $^*P < 0.05$.

To address significance of PLIN5 upregulation in β-cells during fasting and refeeding in an in vivo model that allows the observation within days of PLIN5 upregulation, targeted expression of PLIN5 in β-cells was achieved using AAV-PLIN5 and AAV-GFP as a control (Supplementary Fig. 6*A*–*F*). Weights, blood glucose, serum FA, serum β-hydroxybutyrate, and serum insulin levels were all comparable between AAV-PLIN5 and AAV-GFP mice (Supplementary Fig. 7*A* and *B*). Likewise, IPGTT that bypasses incretin effects and ITT were similar (Fig. 5*C* and Supplementary Fig. 7*C*). Considering that GLP-1 plays a major role in the augmentation of insulin secretion postprandially and activates PKA (37), we tested whether exenatide, a GLP-1R agonist, augments insulin secretion in AAV-PLIN5 mice. After a single dose of exenatide, AAV-PLIN5 mice showed higher sensitivity to exenatide, demonstrating significantly lower glucose levels at early points compared with AAV-GFP control in IPGTT (two-way ANOVA, $P < 0.01$; Fig. 5*D*) along with higher rises in serum insulin (Fig. 5*E*). These data support that PLIN5 expression, as seen during refeeding, augments PP insulin secretion by sensitizing β-cells to the GLP-1 receptor pathway.

DISCUSSION

We previously reported that PLIN2 is an LD protein important for acute augmentation of GSIS by FA in β-cells (14). Here, the localization around LD and promotion of OA uptake into TG establishes PLIN5 as another LD protein in β-cells. However, the two PLINs differ in expression patterns and their regulation of lipid metabolism and insulin secretion, with the implication of PLIN5 in the augmentation of PP insulin secretion. PLIN5 expression is very low during the fed state and increases at mRNA and protein levels during fasting in mouse islets. In comparison, PLIN2 is the predominant LD protein in fed islets. The protein levels of PLIN2 rise modestly (14) without significant increase in mRNA (Fig. 2*B*) in fasted islets, which likely reflects the incorporation of PLIN2 into LD preventing ubiquitin-mediated degradation (Fig. 3*C*) (32). Thus, upregulation of *Plin5* in islets of fasted mice results in quantitative and qualitative changes in the islet LD profile by increasing total TG contents and producing LD tagged with PLIN5 along with PLIN2. The current study indicates that the presence of PLIN5 confers unique metabolic responses to β-cells. Metabolic labeling showed that higher expression of PLIN5 favors lipolysis and FA oxidation in the presence of OA compared with PLIN2 overexpression. Thus, emergence of LD that contains PLIN5 will allow mobilization of lipids for cellular fuel during energy deprivation in β-cells (Fig. 6*A*).

The increase in islet TG during fasting implicates that β-cells capture FA released from adipose tissues beyond their energy needs. The increase in TG during fasting is also reported in heart and liver, two tissues that also upregulate *Plin5* during fasting (20) (Fig. 2*A*). This may be a mechanism to create an intracellular LD depot before the FA supply from adipose tissues declines. In addition, LD that contains PLIN5 formed during fasting may aid PP insulin secretion by providing lipid-derived signaling in response to FA and PKA activation (Fig. 6*B*). PLIN5 but not PLIN2 has been shown to have a PKA consensus sequence and increases lipolysis in response to PKA activation (22). We confirmed that cAMP signaling increases lipolysis in Ad-PLIN5 MIN6 cells and demonstrated that PLIN5 but not PLIN2 amplifies the effects of PA and cAMP signaling on GSIS. To further support the significance of PLIN5 in β-cell physiology, the effects of PLIN5 deficiency or PKA resistance on lipid metabolism and insulin secretion in β-cells need to be explored.

The previous study that modulated PLIN5 expression chronically stressed the role of PLIN5 as a lipolytic barrier (19). The whole-body PLIN5 deletion reduced LD and increased FA oxidation in the heart, whereas PLIN5 overexpression in the heart resulted in cardiac steatosis in mice (20,38,39). In our study, where the effects of PLIN5 overexpression were evaluated within a relatively limited period in β-cells, lipolysis was increased with PLIN5 overexpression despite reduced *ATGL* and *HSL* expressions. The increase in substrates for lipolysis (TG) and the accessibility of these lipases to TG-laden LD may predominantly determine the rate of lipolysis in the context we studied. Lipolysis was further augmented in response to cAMP signaling with PLIN5 overexpression in β-cells. Complex effects of PLIN5 on lipid metabolism are likely due to unique interactions of PLIN5 with multiple lipolytic regulators (19), features also seen with PLIN1, a major regulator of adipose lipolysis (11). PLIN1 prevents lipolysis at the basal state but supports robust lipolysis in a PKA-dependent manner through its interaction with HSL and CGI-58 (11). PLIN5 is highly interactive with ATGL (22,24) and CGI-58 (24) and increases lipolysis in response to PKA activation (22). Indeed, PLIN5 is structurally more homologous to PLIN1 than to PLIN2 (17). The increase in cAMP-dependent lipolysis in PLIN5-expressing cells is modest compared with PLIN1 activation in adipocytes that release FA into circulation to support an energy requirement to the entire body. However, this cAMP-dependent increase in lipolysis mediated by PLIN5 could be sufficient to alter an intracellular profile of lipid metabolites in β-cells to modulate insulin secretion.

That lipolysis regulates gene expression and cellular functions through the generation of signaling metabolites is increasingly recognized. ATGL-knockout mice show massive cardiac steatosis due to reduced FA oxidation from impaired generation of FA that serve as peroxisome proliferator–activated receptor ligands (40). More relevant to islet function are the regulatory roles of lipolysis in the generation of signaling for insulin secretion. HSL, a lipase with high specificity to diacylglycerides (DG), seems to have complex effects on insulin secretion because conflicting phenotypes are reported in mice models with modulation of HSL (8,41). As for ATGL, a lipase responsible for the initial step of lipolysis, its reduction in

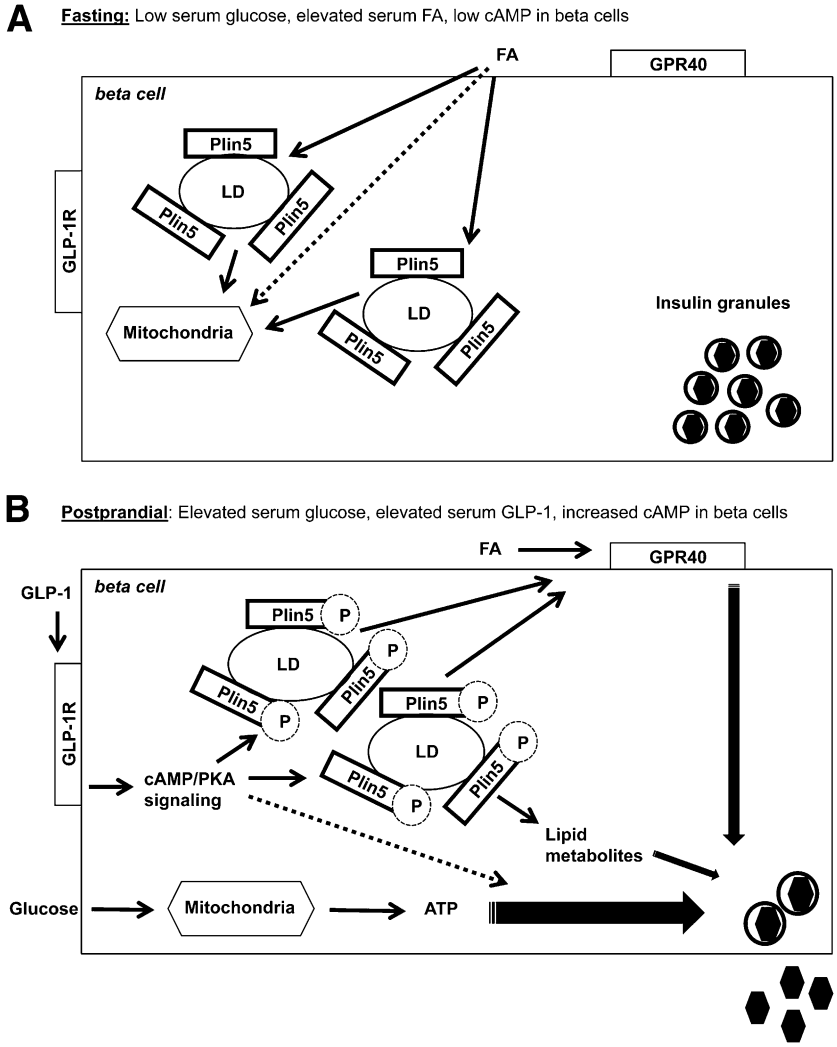

Figure 6—PLIN5 augments PP GSIS through the regulation of lipid handling in β-cells. *A*: On the basis of our results and literature, upregulation of PLIN5 in β-cells during fasting will sequestrate a part of FA influx from the circulation into LD that can be mobilized for β-oxidation in a regulated manner owing to its interaction with mitochondria and lipases. *B*: In addition, LD containing PLIN5 formed during fasting will amplify the augmentation of GSIS by GPR40 and GLP-1R activation, which is likely through the generation of lipolytic signals. PLIN5 is potentially one of the PKA targets and increases lipolysis in response to cAMP. Although PLIN2 is not depicted for clarity of the figure, PLIN2 is another LD protein demonstrated during fed and fasted states in β-cells (14).

insulinoma cells caused broad impairment in insulin secretion in response to glucose, leucine, KCl, and PA (42). Islet-targeted deletion of ATGL reduced GSIS through the impairment of mitochondrial respiration, indicating that basal lipolysis is critical for normal GSIS (43). Here, PLIN5 expression augmented GSIS in the presence of 8-Br-cAMP in a PKA-dependent manner, the condition where PLIN5 increases lipolysis. Thus, the increased expression of PLIN5 during fasting provides a mechanistic basis for the previously documented contribution of FA during fasting for subsequent insulin secretion (9), because PLIN5 will allow β-cells to store FA during fasting and mobilize it for the production of lipolytic signaling to augment GSIS in response to cAMP upon refeeding (Fig. 6). Proposed mediators of lipolytic signaling currently include long-chain acyl-CoA, DG, monoacylglycerol, and ceramides (41,44). β-Cells with PLIN5 expression will provide a model to dissect lipolytic signaling that supports β-cell functions.

Interestingly, the FA augmentation of GSIS by PLIN5 depends heavily on GPR40, a cell surface FA receptor highly expressed in β-cells. It signals predominantly through Gaq/11 that raises $[Ca^{2+}]_i$ and *sn*-1,2 DG. GPR40$^{-/-}$ mice suggest ~50% of FA-mediated augmentation of GSIS depends on GPR40 (7), and a GPR40 agonist is studied as a new type 2 diabetic treatment (45). Our results indicate that intracellular lipolytic signaling generated by PLIN5 also contributes to GPR40 signaling. Thus, PLIN5 may allow β-cells to use FA influx obtained during fasting for GPR40 activation postprandially. PLIN5 may cross talk with the GPR40 pathway extracellularly through the secretion of FA for receptor activation

or by converging with GPR40 signaling intracellularly. Because ATGL generates *sn*-1,3, and *sn*-2,3 DG preferentially (46), the collaboration between PLIN5 and GPR40 will involve mechanisms beyond the simple increase in the *sn*-1,2 DG pool. To add complexity, a GPR40 agonist increased lipolysis and incorporation of FA to DG in insulinoma cells, implying that intracellular lipid metabolism and GPR40 signaling intertwine (47) rather than operate as two separate pathways. Further studies should address whether PLIN5 itself is a molecular target of GPR40 signaling. Likewise, detailed analyses of the insulin secretory pathways through which PLIN5 collaborates with FA and cAMP to augment insulin secretion are warranted, considering FA and cAMP both upregulate GSIS at multiple steps, including exocytosis machineries distal to the rise in $[Ca^{2+}]_i$ (8,35,48).

The current study has high relevance to islet dysfunction in type 2 diabetes by revealing PLIN5 as a potential regulator of PP insulin secretion and providing a model to identify pathways by which lipid signaling supports PP insulin secretion. As other regulators of intracellular lipid metabolism, such as ATGL (43), lipophagy (49), and α/β-hydrolase domain 6 (44) also affect GSIS, indispensability of highly regulated generation of intracellular lipid metabolites for normal β-cell functions is evident. However, what differentiates "healthy" intracellular lipid accumulation from "lipotoxic" accumulation associated with islet dysfunction remains to be determined. Of note, PLIN2 but not PLIN5 expression was increased in islets of high-fat–fed mice at least at transcription levels, indicating chronic overnutrition may favor LD predominantly coated with PLIN2 that are less lipolytic with less interaction with other regulatory factors, including ATGL and mitochondria. Future studies of PLIN2 and PLIN5 under chronic overnutrition may identify roles of islet PLINs in the spatial regulation of lipid metabolism and prevention of "lipotoxic" accumulation.

The tissue-specific study of PLINs is crucial considering the dynamic regulation of PLIN subtype expressions in each tissue. As shown here, *Plin5* and *Plin2* are both upregulated in the liver, whereas only *Plin5* mRNA is increased in islets during fasting. Immunofluorescent analysis of cardiomyocytes showed that PLIN2 and PLIN5 partially colocalize (23), indicating that differential expression of PLINs will create heterogeneous LD within cells. Previous studies (14) and the current study support that PLIN2 and PLIN5 both play roles in lipid metabolism and insulin secretion in β-cells, but with distinct functions. Differential expression of PLIN2 and PLIN5 in β-cells likely serves as a mechanism to organize intracellular lipid metabolism and insulin secretion in response to nutritional cues. However, what regulates differential expression of PLIN5 and PLIN2 in β-cells remains to be determined. The activation of peroxisome proliferator–activated receptor-α and C/EBP-α were previously implicated in the rise of PLIN5 during fasting in the liver (15,50), and their role in the regulation of PLIN5 in β-cells remains to be explored.

In summary, we established that PLIN5 is an LD protein in β-cells whose dynamic expression and interaction with PKA supports lipid metabolism and insulin secretion in response to nutritional cues.

Acknowledgments. The authors thank Amy Ming-Lo Yeh, Emory University, for technical assistance. Human islets were provided for Y.Im. by the Integrated Islet Distribution Program.

Funding. This work was supported by National Institutes of Health grants to Y.Im. (R01-DK-090490 and R01-DK-090490-02W1).

Duality of Interest. D.A.P. is employed by Thermo Fisher. No other potential conflicts of interest relevant to this article were reported.

Author Contributions. M.B.T., Y.M., D.R.H., E.G., and Y.Im. (all aspects), A.C. (GSIS), S.D. and D.A.P. (lipidomics), and Y.Ik. (AAV) were responsible for the acquisition and analysis of the data. M.B.T. and Y.Im. contributed to research design, interpreted the data, drafted the manuscript, and critically revised the manuscript for important intellectual content. All authors revised and approved the final version of the manuscript. Y.Im. conceived the study. Y.Im. is the guarantor of this work and, as such, had full access to all the data in the study and takes responsibility for the integrity of the data and the accuracy of the data analysis.

Prior Presentation. Parts of this study were presented at the FASEB Science Research Conference on Lipid Droplets, Saxtons River, VT, 13–18 July 2014, and the Keystone Symposia on Emerging Concepts and Targets in Islet Biology, Keystone, CO, 6–11 April 2014.

References

1. Weir GC, Bonner-Weir S. Islet β cell mass in diabetes and how it relates to function, birth, and death. Ann N Y Acad Sci 2013;1281:92–105

2. Bonora E, Corrao G, Bagnardi V, et al. Prevalence and correlates of postprandial hyperglycaemia in a large sample of patients with type 2 diabetes mellitus. Diabetologia 2006;49:846–854

3. Monnier L, Colette C, Dunseath GJ, Owens DR. The loss of postprandial glycemic control precedes stepwise deterioration of fasting with worsening diabetes. Diabetes Care 2007;30:263–269

4. Shichiri M, Kishikawa H, Ohkubo Y, Wake N. Long-term results of the Kumamoto Study on optimal diabetes control in type 2 diabetic patients. Diabetes Care 2000;23(Suppl. 2):B21–B29

5. Warnotte C, Gilon P, Nenquin M, Henquin JC. Mechanisms of the stimulation of insulin release by saturated fatty acids. A study of palmitate effects in mouse beta-cells. Diabetes 1994;43:703–711

6. Yaney GC, Corkey BE. Fatty acid metabolism and insulin secretion in pancreatic beta cells. Diabetologia 2003;46:1297–1312

7. Latour MG, Alquier T, Oseid E, et al. GPR40 is necessary but not sufficient for fatty acid stimulation of insulin secretion in vivo. Diabetes 2007;56:1087–1094

8. Prentki M, Matschinsky FM, Madiraju SR. Metabolic signaling in fuel-induced insulin secretion. Cell Metab 2013;18:162–185

9. Dobbins RL, Chester MW, Daniels MB, McGarry JD, Stein DT. Circulating fatty acids are essential for efficient glucose-stimulated insulin secretion after prolonged fasting in humans. Diabetes 1998;47:1613–1618

10. Malaisse WJ, Best L, Kawazu S, Malaisse-Lagae F, Sener A. The stimulus-secretion coupling of glucose-induced insulin release: fuel metabolism in islets deprived of exogenous nutrient. Arch Biochem Biophys 1983;224:102–110

11. Brasaemle DL. Thematic review series: adipocyte biology. The perilipin family of structural lipid droplet proteins: stabilization of lipid droplets and control of lipolysis. J Lipid Res 2007;48:2547–2559

12. Ducharme NA, Bickel PE. Lipid droplets in lipogenesis and lipolysis. Endocrinology 2008;149:942–949

13. Greenberg AS, Coleman RA, Kraemer FB, et al. The role of lipid droplets in metabolic disease in rodents and humans. J Clin Invest 2011;121:2102–2110

14. Faleck DM, Ali K, Roat R, et al. Adipose differentiation-related protein regulates lipids and insulin in pancreatic islets. Am J Physiol Endocrinol Metab 2010;299:E249–E257
15. Dalen KT, Dahl T, Holter E, et al. LSDP5 is a PAT protein specifically expressed in fatty acid oxidizing tissues. Biochim Biophys Acta 2007;1771:210–227
16. Wolins NE, Quaynor BK, Skinner JR, et al. OXPAT/PAT-1 is a PPAR-induced lipid droplet protein that promotes fatty acid utilization. Diabetes 2006;55:3418–3428
17. Yamaguchi T, Matsushita S, Motojima K, Hirose F, Osumi T. MLDP, a novel PAT family protein localized to lipid droplets and enriched in the heart, is regulated by peroxisome proliferator-activated receptor alpha. J Biol Chem 2006; 281:14232–14240
18. Bosma M, Minnaard R, Sparks LM, et al. The lipid droplet coat protein perilipin 5 also localizes to muscle mitochondria. Histochem Cell Biol 2012;137: 205–216
19. Kimmel AR, Sztalryd C. Perilipin 5, a lipid droplet protein adapted to mitochondrial energy utilization. Curr Opin Lipidol 2014;25:110–117
20. Kuramoto K, Okamura T, Yamaguchi T, et al. Perilipin 5, a lipid droplet-binding protein, protects heart from oxidative burden by sequestering fatty acid from excessive oxidation. J Biol Chem 2012;287:23852–23863
21. Li H, Song Y, Zhang LJ, et al. LSDP5 enhances triglyceride storage in hepatocytes by influencing lipolysis and fatty acid β-oxidation of lipid droplets. PLoS One 2012;7:e36712
22. Wang H, Bell M, Sreenivasan U, et al. Unique regulation of adipose triglyceride lipase (ATGL) by perilipin 5, a lipid droplet-associated protein. J Biol Chem 2011;286:15707–15715
23. Granneman JG, Moore HP, Mottillo EP, Zhu Z. Functional interactions between Mldp (LSDP5) and Abhd5 in the control of intracellular lipid accumulation. J Biol Chem 2009;284:3049–3057
24. Granneman JG, Moore HP, Mottillo EP, Zhu Z, Zhou L. Interactions of perilipin-5 (Plin5) with adipose triglyceride lipase. J Biol Chem 2011;286:5126–5135
25. Imai Y, Patel HR, Hawkins EJ, Doliba NM, Matschinsky FM, Ahima RS. Insulin secretion is increased in pancreatic islets of neuropeptide Y-deficient mice. Endocrinology 2007;148:5716–5723
26. Bird SS, Marur VR, Sniatynski MJ, Greenberg HK, Kristal BS. Lipidomics profiling by high-resolution LC-MS and high-energy collisional dissociation fragmentation: focus on characterization of mitochondrial cardiolipins and monolysocardiolipins. Anal Chem 2011;83:940–949
27. Bird SS, Marur VR, Sniatynski MJ, Greenberg HK, Kristal BS. Serum lipidomics profiling using LC-MS and high-energy collisional dissociation fragmentation: focus on triglyceride detection and characterization. Anal Chem 2011; 83:6648–6657
28. Vernier S, Chiu A, Schober J, et al. β-cell metabolic alterations under chronic nutrient overload in rat and human islets. Islets 2012;4:379–392
29. Hsieh K, Lee YK, Londos C, Raaka BM, Dalen KT, Kimmel AR. Perilipin family members preferentially sequester to either triacylglycerol-specific or cholesteryl-ester-specific intracellular lipid storage droplets. J Cell Sci 2012;125: 4067–4076
30. Borg J, Klint C, Wierup N, et al. Perilipin is present in islets of Langerhans and protects against lipotoxicity when overexpressed in the beta-cell line INS-1. Endocrinology 2009;150:3049–3057
31. Thiam AR, Farese RV Jr, Walther TC. The biophysics and cell biology of lipid droplets. Nat Rev Mol Cell Biol 2013;14:775–786
32. Masuda Y, Itabe H, Odaki M, et al. ADRP/adipophilin is degraded through the proteasome-dependent pathway during regression of lipid-storing cells. J Lipid Res 2006;47:87–98
33. Xu G, Sztalryd C, Lu X, et al. Post-translational regulation of adipose differentiation-related protein by the ubiquitin/proteasome pathway. J Biol Chem 2005;280:42841–42847
34. Lavine RL, Voyles N, Perrino PV, Recant L. The effect of fasting on tissue cyclic cAMP and plasma glucagon in the obese hyperglycemic mouse. Endocrinology 1975;97:615–620
35. Tengholm A. Cyclic AMP dynamics in the pancreatic β-cell. Ups J Med Sci 2012;117:355–369
36. Fujiwara K, Maekawa F, Yada T. Oleic acid interacts with GPR40 to induce Ca2+ signaling in rat islet beta-cells: mediation by PLC and L-type Ca2+ channel and link to insulin release. Am J Physiol Endocrinol Metab 2005;289:E670–E677
37. Campbell JE, Drucker DJ. Pharmacology, physiology, and mechanisms of incretin hormone action. Cell Metab 2013;17:819–837
38. Pollak NM, Schweiger M, Jaeger D, et al. Cardiac-specific overexpression of perilipin 5 provokes severe cardiac steatosis via the formation of a lipolytic barrier. J Lipid Res 2013;54:1092–1102
39. Wang H, Sreenivasan U, Gong DW, et al. Cardiomyocyte-specific perilipin 5 overexpression leads to myocardial steatosis and modest cardiac dysfunction. J Lipid Res 2013;54:953–965
40. Haemmerle G, Moustafa T, Woelkart G, et al. ATGL-mediated fat catabolism regulates cardiac mitochondrial function via PPAR-α and PGC-1. Nat Med 2011; 17:1076–1085
41. Prentki M, Madiraju SR. Glycerolipid/free fatty acid cycle and islet β-cell function in health, obesity and diabetes. Mol Cell Endocrinol 2012;353:88–100
42. Peyot ML, Guay C, Latour MG, et al. Adipose triglyceride lipase is implicated in fuel- and non-fuel-stimulated insulin secretion. J Biol Chem 2009;284:16848–16859
43. Tang T, Abbott MJ, Ahmadian M, Lopes AB, Wang Y, Sul HS. Desnutrin/ATGL activates PPARδ to promote mitochondrial function for insulin secretion in islet β cells. Cell Metab 2013;18:883–895
44. Zhao S, Mugabo Y, Iglesias J, et al. α/β-Hydrolase domain-6-accessible monoacylglycerol controls glucose-stimulated insulin secretion. Cell Metab 2014; 19:993–1007
45. Burant CF. Activation of GPR40 as a therapeutic target for the treatment of type 2 diabetes. Diabetes Care 2013;36(Suppl. 2):S175–S179
46. Eichmann TO, Kumari M, Haas JT, et al. Studies on the substrate and stereo/regioselectivity of adipose triglyceride lipase, hormone-sensitive lipase, and diacylglycerol-O-acyltransferases. J Biol Chem 2012;287:41446–41457
47. El-Azzouny M, Evans CR, Treutelaar MK, Kennedy RT, Burant CF. Increased glucose metabolism and glycerolipid formation by fatty acids and GPR40 receptor signaling underlies the fatty acid potentiation of insulin secretion. J Biol Chem 2014;289:13575–13588
48. Kaihara KA, Dickson LM, Jacobson DA, et al. β-Cell-specific protein kinase A activation enhances the efficiency of glucose control by increasing acute-phase insulin secretion. Diabetes 2013;62:1527–1536
49. Pearson GL, Mellett N, Chu KY, et al. Lysosomal acid lipase and lipophagy are constitutive negative regulators of glucose-stimulated insulin secretion from pancreatic beta cells. Diabetologia 2014;57:129–139
50. Zhou L, Zhang L, Meng Q, et al. C/EBPα promotes transcription of the porcine perilipin5 gene. Mol Cell Endocrinol 2012;364:28–35